Applied Mathematical Modelling 47 (2017) 96–102

Contents lists available at ScienceDirect

Applied Mathematical Modelling

journal homepage: www.elsevier.com/locate/apm

Quasi-analytical solution of two-dimensional Helmholtz equation

A. Van Hirtum

GIPSA-lab, UMR CNRS 5216, Université Grenoble Alpes, Grenoble, France

ARTICLE INFO

Article history:
Received 29 March 2016
Revised 24 January 2017
Accepted 15 March 2017
Available online 20 March 2017

Keywords:
Transformed Helmholtz equation
Conformal mapping

ABSTRACT

The two-dimensional Helmholtz differential equation governs vibrational problems for a thin membrane and is therefore well studied. Analytical solutions are limited to particular domain shapes, so that in general numerical methods are used when an arbitrary domain is considered. In this paper, a quasi-analytical solution is proposed, suitable to be applied to an arbitrary domain shape. Concretely, the Helmholtz equation is transformed to account for a conformal map between the shape of the physical domain and the unit disk as canonical domain. This way, the transformed Helmholtz equation is solved exploiting well known analytical solutions for a circular domain and the solution in the physical domain is obtained by applying the conformal map. The quasi-analytical approach is compared to analytical solutions for the case of a circular, elliptic and squared domain.

1. Introduction

The reduced Helmholtz equation is an elliptic differential equation allowing to describe physical phenomena related to oscillatory problems. As such, it is a classical problem for diverse fields of physics and engineering such as vibration mechanics, electro-magnetics, acoustics or quantum mechanics [1–3]. Solution of the two-dimensional (2D) Helmholtz equation allows to identify vibration modes for a two-dimensional domain. Analytical solutions are limited to domains with a particular shape such as a rectangle or circle [2,4]. In general, solving this differential equation relies on numerical methods, see e.g. [5–9].

In the current work, a quasi-analytical solution of the two-dimensional Helmholtz equation is sought. A quasi-analytical method is preferred when a computationally low-cost solution is of interest or when an analytical model approach is preferred.

In the following, the quasi-analytical approach is outlined and obtained solutions are compared with analytical solutions for a circular, elliptic and squared domain.

2. Transformed Helmholtz equation

The two-dimensional (2D) spatial Helmholtz equation in Cartesian coordinates for $P(x, y)$ is defined as:

$$\frac{\partial^2 P}{\partial x^2} + \frac{\partial^2 P}{\partial y^2} + \alpha^2 P = 0, \tag{1}$$

E-mail address: annemie.vanhirtum@grenoble-inp.fr

http://dx.doi.org/10.1016/j.apm.2017.03.026
0307-904X/

where (x, y) corresponds to the two-dimensional physical plane and α indicates the wavenumber. Solution of (1) is sought at the interior of a region $\mathcal{D}$ bounded by a closed curve $\mathcal{C}$. Moreover, we consider hard wall boundaries so that Neumann boundary condition applies on the boundary $\mathcal{C}$:

$$\left.\frac{\partial P}{\partial \mathbf{n}}\right|_{\mathcal{C}} = 0, \tag{2}$$

with $\mathbf{n}$ denoting the normal to boundary $\mathcal{C}$.

The Helmholtz Eq. (1) is then expressed as function of complex variable $w = x + \imath y$ and its complex conjugate $\overline{w} = x - \imath y$. The Laplace operator becomes:

$$dw = dx + \imath dy \quad \text{and} \quad \frac{\partial^2}{\partial x^2} + \frac{\partial^2}{\partial y^2} = 4\frac{\partial^2}{\partial w \partial \overline{w}}, \tag{3}$$

so that the expression of the Helmholtz equation in the $(w, \overline{w})$ plane is given as:

$$\frac{\partial^2 P}{\partial w \partial \overline{w}} + \frac{1}{4}\alpha^2 P = 0. \tag{4}$$

In order to solve (4) quasi-analytically, the physical $(w, \overline{w})$ plane is mapped to the canonical plane introducing mapping function

$$w = f(s), \tag{5}$$

with $s = u + \imath v$ and $\bar{s} = u - \imath v$ again its complex conjugate. Consequently, $dw = f'(s)ds$ holds , corresponding to an expansion of factor $|f'(s)|$ and a rotation with angle $\arg(f'(s))$. The Laplace operator in the physical plane (3) is in canonical plane $(s, \bar{s})$ expressed as:

$$4\frac{\partial^2}{\partial w \partial \overline{w}} = 4\frac{1}{f'(s)\overline{f'(s)}}\frac{\partial^2}{\partial s \partial \bar{s}}. \tag{6}$$

Since $f'(s)\overline{f'(s)} = |f'(s)|^2$ holds, the transformed Helmholtz equation in the canonical plane is then written as:

$$\frac{\partial^2 P}{\partial s \partial \bar{s}} + \frac{|f'(s)|^2}{4}\alpha^2 P = 0. \tag{7}$$

Instead of solving the original Eq. (1), the transformed Eq. (7) is solved by rewriting it as:

$$\frac{\partial^2 P}{\partial s \partial \bar{s}} - \left(\frac{\imath\alpha}{2}\right)^2 f'(s)\overline{f'(s)}P = 0, \tag{8}$$

and applying separation of variables $P = P_1(s)P_2(\bar{s})$. This results in

$$P_1{}'P_2{}' - \left(\frac{\imath\alpha}{2}\right)^2 f'(s)\overline{f'(s)}P_1P_2 = 0, \tag{9}$$

and therefore in two first order differential equations where τ denotes the separation constant:

$$\begin{aligned} P_1{}' - \left(\frac{\imath\alpha}{2}\right)\tau f'(s)P_1 &= 0, \\ P_2{}' - \left(\frac{\imath\alpha}{2}\right)\frac{1}{\tau}\overline{f'(s)}P_2 &= 0. \end{aligned} \tag{10}$$

Solutions for $P_1(s)$ and $P_2(\bar{s})$ are then of the form

$$\begin{aligned} P_1 &= c_1 e^{\imath\tau\frac{\alpha}{2}f(s)}, \\ P_2 &= c_2 e^{\frac{\imath}{\tau}\frac{\alpha}{2}\overline{f(s)}}. \end{aligned} \tag{11}$$

The general solution of (7) is then given as a linear combination of the products of P_1 and P_2 corresponding to various values of τ [10]:

$$P(s, \bar{s}) = \int_W A(\tau) e^{\imath\alpha[\tau f(s) + \overline{f(s)}/\tau]\frac{1}{2}} d\tau, \tag{12}$$

with W any path in the τ-space which makes the expression convergent [10,11]. Let us further put $\tau = \exp(-\imath\eta)$ and $f(s) = |f(s)|\exp(\imath\chi)$ with $\eta \in \mathbb{C}$ a complex number, norm $|f|$ and χ denoting the phase angle of $f(s)$. Substituting these notations in (12) and denoting $\kappa = \eta - \chi - \frac{\pi}{2}$ results in

$$P(s, \bar{s}) = -\int_W A(e^{-\imath\eta}) e^{-\imath\alpha|f|\sin(\kappa)} e^{-\imath\kappa} e^{-\imath\chi} d\kappa. \tag{13}$$

Introducing arbitrary constants a_m with $m \in \mathbb{Z}$ and exploiting periodicity yields

$$P(s,\bar{s}) = \sum_{m=-\infty}^{+\infty} a_m e^{\imath m\chi} \int_W e^{\imath m\kappa - \imath\alpha|f|\sin(\kappa)} d\kappa. \tag{14}$$

This expression can be simplified introducing $H_m(\alpha \cdot |f|) = \int_W e^{\imath m\kappa - \imath\alpha|f|\sin(\kappa)} d\kappa$:

$$P(s,\bar{s}) = \sum_{m=-\infty}^{+\infty} a_m e^{\imath m\chi} H_m(\alpha \cdot |f|), \tag{15}$$

which using the definition of χ becomes

$$P(s,\bar{s}) = \sum_{m=-\infty}^{+\infty} a_m H_m(\alpha \cdot |f|) \left[\frac{f(s)}{|f(s)|}\right]^m. \tag{16}$$

Eq. (16) provides the general solution of the transformed two-dimensional spatial Helmholtz equation.

3. Solution of transformed Helmholtz equation using conformal mapping

When the unit disk is taken as canonical plane, (16) can be formulated using cylindrical functions as $H_m(\alpha \cdot |f|) = J_m(\alpha \cdot |f|)$, with J_m denoting Bessel function of the first kind with order m and with mapping function $\alpha \cdot |f|$ as its argument. From hard wall boundary condition (2) and general solution (16) follows then that:

$$\left.\frac{\partial J_m(\alpha \cdot |f|)}{\partial \mathbf{n}}\right|_{\mathcal{C}} = 0, \tag{17}$$

holds, which can only be satisfied for discrete values corresponding to the roots of the derivative of Bessel function of order m so that $\alpha = \alpha_{ml}$ with $l = 0, 1, 2, \ldots$ The general solution of the transformed Helmholtz equation on the unit disk (16) becomes:

$$P(s,\bar{s}) = \sum_{m=-\infty}^{+\infty} a_m J_m(\alpha_{ml} \cdot |f|) \left[\frac{f(s)}{|f(s)|}\right]^m, \tag{18}$$

with $l = 0, 1, 2, \ldots$ This way (16) can be solved once mapping function f is determined. In the following Section 4, the approach is applied to domains for which an analytical solution of the 2D Helmholtz equation is known.

4. Application to a circular, elliptic and squared domain

In the following, we apply the approach outlined in Section 3 to physical domain shapes, for which a mapping function (5) can be formulated so that solutions of (18) can be compared with well known analytical solutions of the Helmholtz equation such as on the interior of a circular, elliptic or squared domain [2]. Wavenumbers $\alpha_{m,l}$ are obtained from (17) so that associated cut-off frequencies are obtained using the relationship

$$f_{m,l} = \frac{\alpha_{m,l} \cdot c}{2\pi}, \tag{19}$$

so that for given wave velocity c, cut-off frequencies are determined as:

$$f_{m,l} = \left.\frac{\chi_{m,l} \cdot c}{2\pi \cdot |f(s)|}\right|_{\mathcal{C}}, \tag{20}$$

with $\chi_{m,l} = \alpha_{m,l} \cdot |f(s)|_{\mathcal{C}}$ denoting zeros of the derivative of the Bessel function of order m on the boundary of the physical domain as expressed by (20). Zero values are well studied and can be obtained in several ways, from tables, using recursive formulas or iteratively using Newton–Raphson as applied here [10,12,13]. Except for $(m,l) = (0,0)$ for which $\chi_{0,0} = 0$, values $\chi_{m,l} > 1$ as illustrated in Fig. 1 where $\chi_{m,l}$ is plotted in increasing order.

4.1. Circular physical domain

When the physical domain is the interior of a circle with radius $R > 0$, the conformal mapping function $w = f(s)$ is expressed as $w = R \times s$. When polar coordinates (ρ, θ) are used to describe the unit circle in the canonical plane, *i.e.* $s = \rho \exp(\imath\theta)$, solution (18) becomes:

$$P(s,\bar{s}) = \sum_{m=-\infty}^{+\infty} a_m J_m(\alpha_{ml} \cdot R \cdot \rho) e^{\imath m\theta}, \tag{21}$$

and associated cut-off frequencies (20) yield:

$$f_{m,l} = \frac{\chi_{m,l} \cdot c}{2\pi R}, \tag{22}$$

matching analytical values [2].

Resulting solutions mapped on the circle with radius $R = 12.5$ mm are illustrated in Fig. 2.

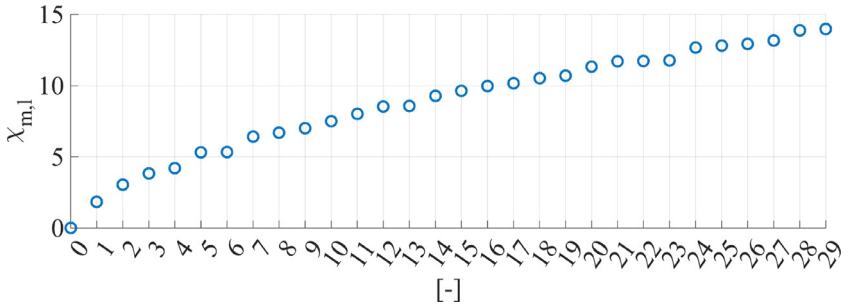

Fig. 1. Illustration of zeros $\chi_{m,l}$ of the derivative of the Bessel function sorted in increasing order.

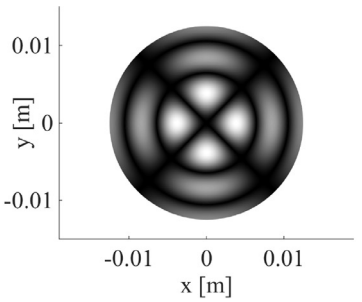

(a) $(m,l) = (2,2)$

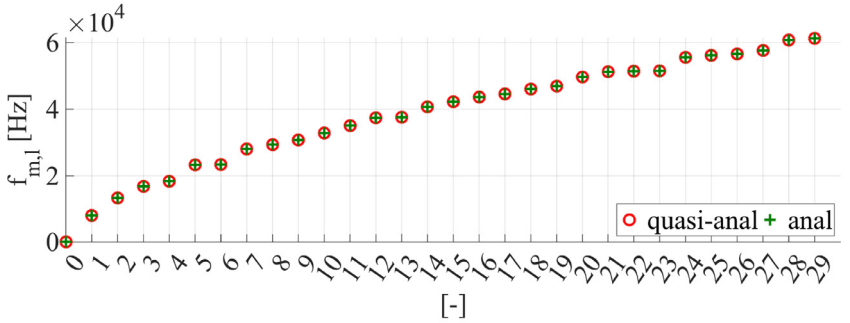

(b) sorted $f_{m,l}$

Fig. 2. Illustration of 2D Helmholtz equation for a circular domain with radius $R = 12.5$ mm: (a) solution for $(m,l) = (2,2)$ and (b) sorted cut-off frequencies $f_{m,l}$ for wave velocity $c = 344$ m/s from (20) (quasi-anal, ○) and from (22) (anal, +).

4.2. Elliptic physical domain

When the physical domain is the interior of an ellipse with major semi-axis a and minor semi-axis b ($a \geq b > 0$), the common Joukowski function [14] provides a conformal mapping function $w = f(s)$ as:

$$w = \frac{1}{2}\rho\left(\mathcal{R}e^{\imath\theta} + \frac{\lambda^2}{\mathcal{R}e^{\imath\theta}}\right), \tag{23}$$

$$= \frac{1}{2}\rho\left(\mathcal{R} + \frac{\lambda^2}{\mathcal{R}}\right)\cos\theta + \imath\frac{1}{2}\rho\left(\mathcal{R} - \frac{\lambda^2}{\mathcal{R}}\right)\sin\theta, \tag{24}$$

with parameters $(\lambda, \mathcal{R})$ are directly derived from the semi-axes (a, b) of the ellipse as: $\mathcal{R} = a + b > 0$ and $\lambda^2 = a^2 - b^2$ and (ρ, θ) corresponds again to polar coordinates used to describe the unit disk in the canonical plane. Note that λ indicates the focal distance of the ellipse and that $\lambda^2 < \mathcal{R}$ follows from $a \geq b > 0$.

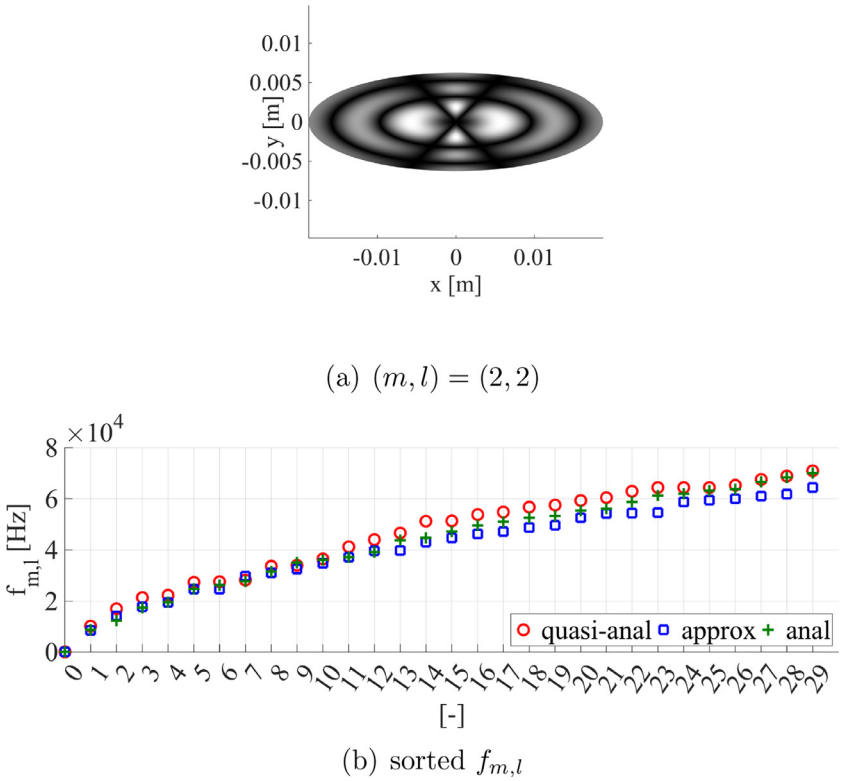

Fig. 3. Illustration of 2D Helmholtz equation for an elliptic domain with major semi-axis $a = 18.8$ mm and minor semi-axis $b = 6.2$ mm: (a) solution for $(m, l) = (2, 2)$ and (b) sorted cut-off frequencies $f_{m,l}$ for wave velocity $c = 344$ m/s from (20) (quasi-anal, ○), from (26) with $\beta_{el} = 0.7$ (approx, □) and from (27) (anal, +).

Solution (18) is then expressed as:

$$P(s,\bar{s}) = \sum_{m=-\infty}^{+\infty} a_m J_m\left(\alpha_{ml}\cdot\frac{1}{2}\left(\mathcal{R}^2+\frac{\lambda^4}{\mathcal{R}^2}+2\lambda^2\cos(2\theta)\right)^{1/2}\cdot\rho\right) \cdot\left[\frac{\mathcal{R}e^{\imath\theta}+\frac{\lambda^2}{\mathcal{R}}e^{-\imath\theta}}{\left(\mathcal{R}^2+\frac{\lambda^4}{\mathcal{R}^2}+2\lambda^2\cos(2\theta)\right)^{1/2}}\right]^m, \tag{25}$$

and associated cut-off frequencies (20) are approximated as:

$$f_{m,l} \approx \frac{\chi_{m,l}\cdot c}{\pi\beta_{el}\mathcal{R}}, \tag{26}$$

where $\mathcal{R}/2$ corresponds to the mean value between $\min(|f|_C) = \frac{1}{2}\left(\mathcal{R}-\frac{\lambda^2}{\mathcal{R}}\right)$ and $\max(|f|_C) = \frac{1}{2}\left(\mathcal{R}+\frac{\lambda^2}{\mathcal{R}}\right)$ and $\beta_{el}(b/a)$ denotes a proportionality coefficient whose value depends on the aspect ratio of the semi-axes of the ellipse b/a.

Analytical values of the cut-off frequencies for the elliptic domain are given as [15–17]:

$$f_{p,r} = \frac{c}{\pi}\sqrt{\frac{q_{p,r}}{\lambda^2}}, \tag{27}$$

with $q_{p,r}$ the rth zero of the radial or modified Mathieu function of order p.

Solutions mapped on an elliptic domain with major semi-axis $a = 18.8$ mm and minor semi-axis $b = 6.2$ mm, *i.e.* $b/a = 0.3$, are illustrated in Fig. 3. Sorted cut-off frequencies estimated using (26) with $\beta_{el} = 0.7$ are on average within 4% of analytical values obtained using (27). However, the accuracy of the approximation depends on the chosen value of β_{el}. This is illustrated in Fig. 4(a) where the mean error $\Delta f_{m,l}$ of the 10 lowest approximated cut-off frequencies with respect to analytical values is plotted as a function of semi-axes aspect ratio b/a. When a single β_{el}-value is used regardless of the semi-axes ratio a minimum error is indeed observed as illustrated for $\beta_{el} = 0.7$ and $\beta_{el} = 0.8$ in Fig. 4(a). When β_{el} is

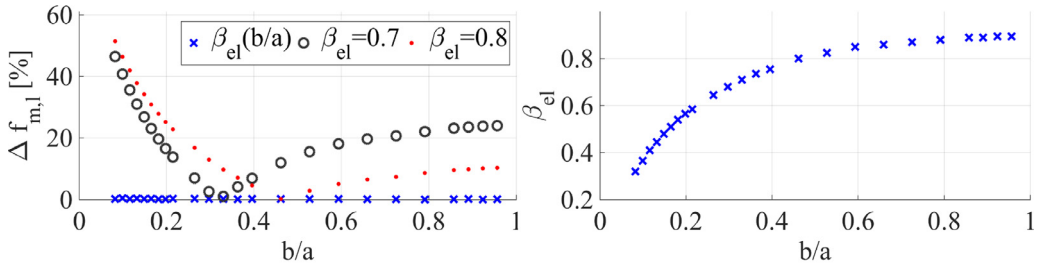

(a) $\Delta f_{m,l}(b/a)$ (b) $\beta_{el}(b/a)$

Fig. 4. (a) Mean error $\Delta f_{m,l}(b/a)$ of approximated (26) compared to analytical (27) sorted cut-off frequencies for different β_{el}. (b) $\beta_{el}(b/a)$ minimizing $\Delta f_{m,l}(b/a) < 1\%$.

optimized as a function of the semi-axes ratio b/a, the error is less than 4% for the assessed range of aspect ratios $0.05 < b/a < 1$.

Optimized $\beta_{el}(b/a)$ values are plotted in Fig. 4(b). Optimal values $0.3 < \beta_{el} < 0.9$ increase with aspect ratio b/a. Moreover, for $0.3 < b/a < 1$, the range of optimal β_{el} values is comprised within $0.7 < \beta_{el} < 0.9$, so that when $\beta_{el} = 0.8$ is used within this range ($0.3 < b/a < 1$) the error (Fig. 4(a)) remains limited (<10%) whereas outside this range the error increases rapidly (up to more than 40%). Optimal $\beta_{el}(b/a)$ shown in Fig. 4(b) can be fitted so that cut-off frequencies can be approximated (Fig. 4(a)) to within 4% of analytical values (27) for the lowest 10 cut-off frequencies and to within 15% thereafter. Quasi-analytical cut-off frequencies (20) are estimated to within 5% of analytical values (27).

4.3. Squared physical domain

When the physical domain is the interior of a square with side length $2a > 0$, *i.e.* domain $[-a, a] \times [-a, a]$, the following conformal map $w = f(s)$ is applied [18]:

$$w = \left[\Re\left(-\frac{1-\imath}{K_e}F\left(\cos^{-1}\left(\frac{1+\imath}{\sqrt{2}}s\right)\right), \frac{1}{\sqrt{2}}\right)+1\right]\cdot a + \imath\left[\Im\left(-\frac{1-\imath}{K_e}F\left(\cos^{-1}\left(\frac{1+\imath}{\sqrt{2}}s\right)\right), \frac{1}{\sqrt{2}}\right)-1\right]\cdot a, \tag{28}$$

with Legendre elliptic integral with modulus $k = 1/\sqrt{2}$

$$F(\phi, k) = \int_0^{\phi} \frac{dt}{\sqrt{1-k^2\sin^2 t}}. \tag{29}$$

and $K_e \approx 1.854$ the value of the complete integral with same modulus. Associated cut-off frequencies (20) are approximated as:

$$f_{m,l} \approx \frac{\chi_{m,l}\cdot c}{2\pi a \beta_{sq}}, \tag{30}$$

with $f(s)|_{\mathcal{C}} \approx a \cdot \beta_{sq}$ and $\beta_{sq} = 1.2$ taken as the mean value between $\min(|f|_{\mathcal{C}}/a) = 1$ and $\max(|f|_{\mathcal{C}}/a) = \sqrt{2}$.

Analytical values of the cut-off frequencies for the square yield [2]

$$f_{p,r} = \frac{c}{4a}\sqrt{p^2+r^2}. \tag{31}$$

Resulting solutions mapped on a squared domain are illustrated in Fig. 5. Approximated cut-off frequencies (30) and quasi- analytical estimations (20) are on average respectively within 4% and 8% of analytical values (31).

5. Conclusion

A quasi-analytical method to solve the two-dimensional spatial Helmholtz equation is proposed and applied to a circular, squared and elliptic physical domain. It is shown that the first 30 modal cut-off frequencies can be estimated using the quasi-analytical approach. Compared to analytical values, the estimation is exact for a circular domain and has a mean accuracy to within 5% for the elliptic domain and to within 8% for the squared domain for the lowest 29 cut-off frequencies. Moreover, for the squared and elliptic domain an approximation of cut-off frequencies is given which has compared to analytical values a mean accuracy to within 4% for the elliptic domain and to within 5% for the squared domain for the lowest 10 cut-off frequencies. The analytical expression for a squared domain is straightforward so that the given approximation can be considered superfluous. In the case of an elliptic domain, the proposed approximation provides a straightforward estimation of the first cut-off frequencies avoiding the use of cumbersome Mathieu functions involved in the analytical expression. The proposed approach can be applied to two-dimensional domains with a different boundary shape using *e.g.* the Schwarz–Christoffel transformation to map the unit disk to the domain in the physical plane.

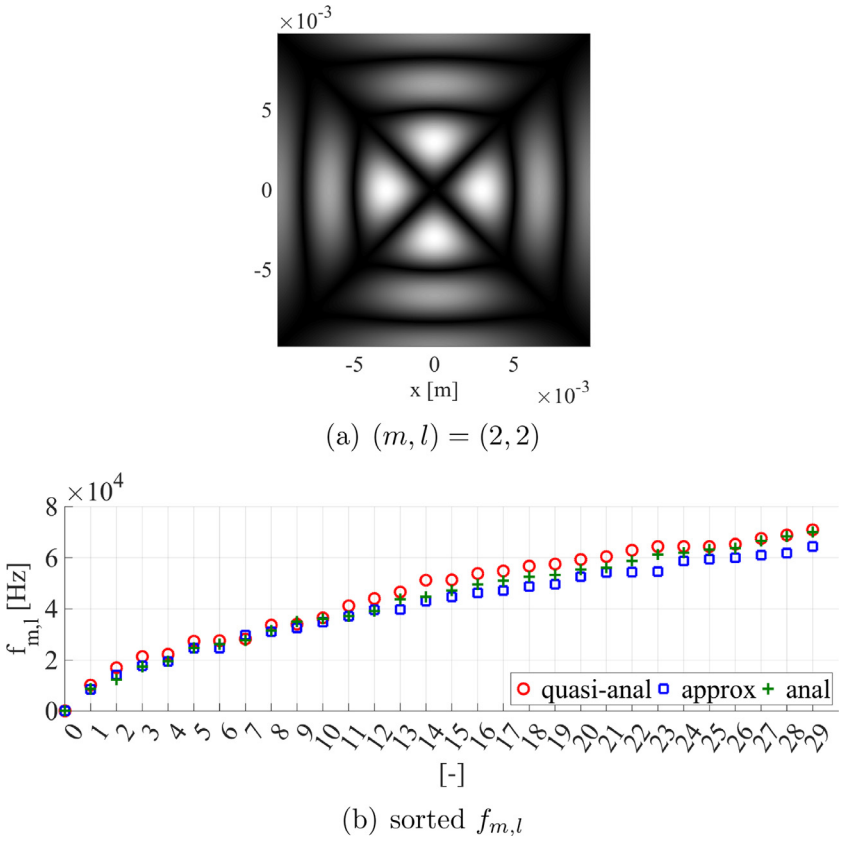

Fig. 5. Illustration of 2D Helmholtz equation for a squared domain with half-side length $a = 9.8$ mm: (a) solution for $(m, l) = (2, 2)$ and (b) sorted cut-off frequencies $f_{m,l}$ for wave velocity $c = 344$ m/s from (20) (quasi-anal, ∘), from (30) (approx, □) and from (31) (anal, +).

Acknowledgments

This work was partly supported by EU-FET grant (EUNISON 308874) and ANR ArtSpeech (ANR-15-CE23-0024). Phon Vu Tran is acknowledged for helpful discussion.

References

[1] L. Chu, Electromagnetic waves in elliptic hollow pipes of metal, J. Appl. Phys. 9 (1938) 583–591.
[2] D. Jones, Acoustic and Electromagnetic Waves, Clarendon Press, Oxford, UK, 1989.
[3] M. Porter, R. Liboff, Vibrating quantum billiards on Riemannian manifolds, Int. J. Bifurc. Chaos 11 (9) (2001) 2305–2315.
[4] G. Gladwell, N. Willms, On the mode shapes of the Helmholtz equation, J. Sound Vib. 188 (3) (1995) 419–433.
[5] A. Bayliss, C. Goldstein, The numerical solution of the Helmholtz equation for wave propagation problems in underwater acoustics, Comput. Math. Appl. 11 (1985) 655–665.
[6] H. Wilson, R. Scharstein, Computing elliptic membrane high frequencies by Mathieu and Galerkin methods, J. Eng. Math. 57 (2007) 41–55.
[7] C. Tsai, D. Young, C. Chiu, C. Fan, Numerical analysis of acoustic modes using the linear least squares method of fundamental solutions, J. Sound Vib. 324 (2009) 1086–1110.
[8] S. Rienstra, W. Eversman, A numerical comparison between the multiple-scales and finite-element solution for sound propagation in lined flow ducts, J. Fluid Mech. 437 (2001) 367–384.
[9] Y. Wong, G. Li, Exact finite difference schemes for solving Helmholtz equation at any wavenumber, Int. J. Numer. Anal. Model. 2 (1) (2011) 91–108.
[10] B. Gupta, Mathematical Physics, Vikas Publishing House, India, 2002.
[11] D. Liu, B. Gai, G. Tao, Applications of the method of complex functions to dynamic stress concentrations, Wave Motion 4 (1982) 293–304.
[12] M. Abramowitz, I. Stegun, Handbook of Mathematical Functions, U.S. Government Printing Office, Washington, 1972.
[13] G. Morgenthaler, H. Reismann, Zeros of first derivatives of Bessel functions of the first kind, J. Res. Natl. Bur. Stand. 67B (1963) 181–183.
[14] H. Malonek, R. De Almeida, A note on a generalized Joukowski transformation, Appl. Math. Lett. 23 (2010) 1174–1178.
[15] G. Chen, P. Morris, J. Zhou, Visualisation of special eigenmode shapes of a vibrating elliptical membrane, SIAM Rev. 36 (1994) 453–469.
[16] J. Guitierrez-Vega, R. Rodriguez-Dagnino, Mathieu functions, a visual approach, Am. J. Phys. 71 (2003) 233–242.
[17] B. Troesch, H. Troesch, Eigenfrequencies of an elliptic membrane, Math. Comput. 27 (124) (1973) 755–765.
[18] N. Papamichael, C. Kokkinos, M. Warby, Numerical techniques for conformal mapping onto a rectangle, J. Comput. Appl. Math. 20 (1987) 349–358.